J2.4. THE MADDEN JULIAN OSCILLATION: IDENTIFICATION

Michael J. Ventrice
Weather Service International,
Andover, MA

Matthew C. Wheeler
Centre for Australian Weather and Climate Research, Bureau of Meteorology,
Melbourne, Australia

Harry H. Hendon
Centre for Australian Weather and Climate Research, Bureau of Meteorology,
Melbourne, Australia

Carl J. Schreck III
Cooperative Institute for Climate and Satellites (CICS-NC),
North Carolina State University, Asheville, North Carolina
NOAA-National Climatic Data Center, Asheville, North Carolina

Chris D. Thorncroft
Department of Atmospheric and Environmental Science, University at Albany,
Albany, NY

George N. Kiladis
Physical Sciences Division,
NOAA/Earth System Research Laboratory
Boulder, CO

1. Introduction

It is now well known that the Madden Julian Oscillation (MJO) is the main driver of large-scale variations of convection in the tropics. In addition to playing a large role in the tropics, the MJO can also influence extra-tropical circulation. This tropical-extra-tropical relationship makes knowing the state of the MJO in a real-time operational environment very important to medium-range and seasonal forecasters.

While the popular real-time multivariate MJO indices (RMM) have been created in order to monitor the location and intensity of the MJO in real-time operations, this particular MJO index can sometimes struggle during particular seasons and particular base states with correctly identifying the current state of the MJO.

It is evident that we need to continue to develop new MJO indices to overcome certain deficiencies in our tools to monitor the MJO. One such attempt is a newly built MJO index, similar to the RMM indices, but excludes the convection component of the MJO (i.e. outgoing long wave radiation) and focuses more so on the circulation component of the MJO. Thus, this new MJO index is derived of velocity potential at 200 hPa (VP200), as well as zonal winds in both the lower and upper troposphere (U200 & U850). This particular MJO index has been denoted as the Velocity Potential MJO (VPM) indices.

*Corresponding Author Address: Michael J. Ventrice
Weather Service International
400 Minuteman Road, Andover, MA 01810
Email: Michael.Ventrice@weather.com

2. The VPM vs. RMM Indices

The spatial structures (eigenvector) of the leading three EOFs of the combined fields of U200, U850, and VP200 are shown in Fig. 1. The explained variances (eigenvalues) of EOF1 (22%) and EOF2 (20%) are similar and suggestive of a pair. Taking the first two EOFs as a pair, their summed explained variance is 42.5%, while EOF3 explains only 6.8% of the variance. Therefore the first two EOFs are well separated from the third. noisy than OLR.

The summed variance of EOF1 and EOF2 from the RMM EOFs explain only 25% of the variance. The higher explained variance here for the VPM EOFs is attributed to the use of VP200, which is much less spatially and temporally noisy than OLR.

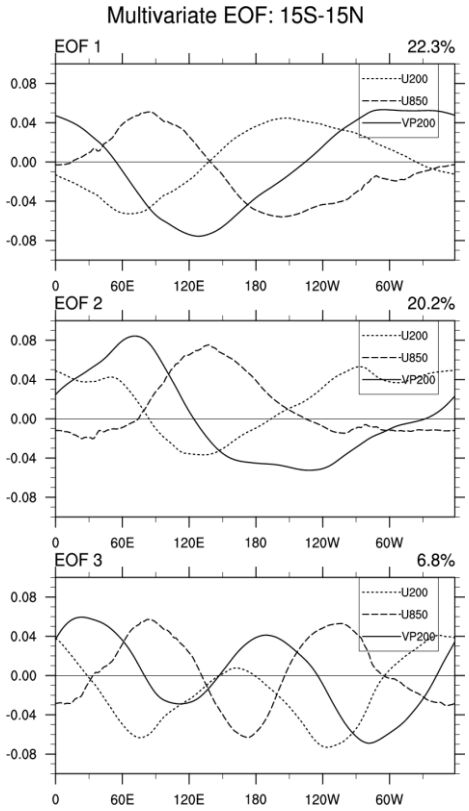

FIG. 1 Spatial structures of EOFs 1, 2, and 3 of the combined analysis of anomalous U200, 4 U850, and VP200.

The cross-power spectrum of the PCs is another way to verify that the leading EOFs are a pair that describes the eastward propagating characteristics of the MJO.

Figure 2 shows the coherence squared (Coh^2) of the leading pair of VPM PCs and that of the original RMM PCs for comparison. The Coh^2 between the new PCs peaks in the 30-80 day range, with a mean value of 0.84 and a phase lag of ¼ cycle (i.e. PC1 leads PC2 by 15 days, not shown), confirming that the leading pair of the VPM EOFs is depicting coherent eastward propagation.

The corresponding Coh^2 for the original RMM indices is 0.78, also with a phase lag of ¼ cycle. Hence, both the new and old leading pair of EOFs describe a similar eastward propagation of the MJO, although with slightly more coherence in the VPM PCs.

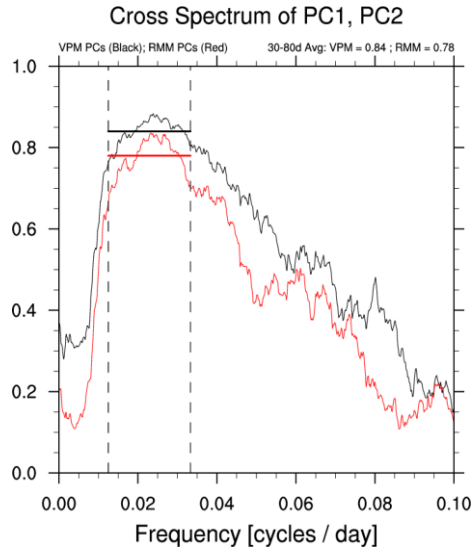

FIG. 2. Coherence squared between PC1 and PC2 of the VPM EOF analysis (black line) and between PC1 and PC2 of the RMM EOF analysis (red line).

To compare the behavior of the VPM and RMM EOFs in identifying the MJO, Fig. 3 shows the total number of days when the index amplitude ≥ 1 (defined as an "MJO day") for all MJOs phases during all months (top), only boreal winter months (middle), and only boreal summer months (bottom). While we define an MJO day as a date where the index is greater than one sigma, it should be noted that there are times when the index can temporarily be greater than one sigma when no coherent MJO signal is present. This often occurs during times where noise (i.e., extratropical waves, convectively coupled atmospheric Kelvin waves, or equatorial Rossby waves) unrelated to the MJO project onto the PCs.

To begin, there are a total of 38 more MJO days using the VPM index rather than RMM in the 1990-2009 climatology. While the differences are subtle, the VPM captures a higher number of MJO days during phases 3, 5, 6, 7, and 8 when compared to RMM. This result is indicative of increased MJO identification by the VPM index, especially over the Pacific and Atlantic basins.

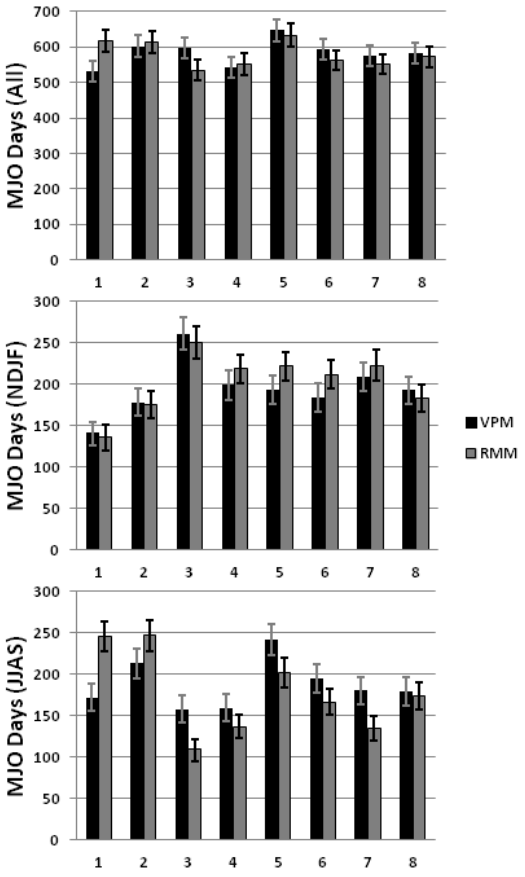

FIG. 3. The number of MJO days, defined as a day where the amplitude for the VPM (black) or RMM (grey) index was greater than or equal to 1 standard deviation, binned for all MJO phases during all months (top); boreal winter (November – February) only months (middle); boreal summer (June-September) only months. The 90% confidence interval is indicated by the error bars.

After dividing the number of MJO days for only boreal winter (November – February), the RMM captures a total of 61 more MJO days when compared to VPM. The increased number of boreal winter MJO days identified by RMM is during times when the MJO is located over the Maritime Continent and West Pacific (phases 4-7). This is a time when the South Pacific Convergence Zone becomes convectively active, thus indicating a benefit of using OLR over VP200. However, note that there are slightly more boreal winter MJO days over the Western Hemisphere and Indian Ocean (phases 8, 1, and 2) using VPM over RMM, suggesting that the VPM is capturing a slightly stronger Western Hemisphere MJO signal over RMM.

For boreal summer (June – September), an opposite relationship is found (with exception of the Western Hemisphere), where there are 85 more MJO days identified using VPM when compared to RMM.

The VPM index captures more MJO days in all phases except when the MJO is present over the Indian Ocean (phases 1-2). This result suggests a potential use for the VPM index with regards to the Summer Monsoons, as well as tropical cyclone activity over the West and East Pacific, and the Atlantic basins.

3. Atlantic tropical cyclone statistics

To investigate the possible enhanced utility of the VPM EOFs to detect the modulation of Atlantic tropical cyclones by the MJO, we count all tropical cyclones that developed during June-September when the amplitude ≥ 1 and then we binned them by each phase of the MJO (Fig. 4a). We do this using both the VPM PCs and the original RMM indices. Tropical cyclogenesis is defined as the time when the National Hurricane Center classified a tropical cyclone as a tropical storm (sustained maximum winds of 34 knots).

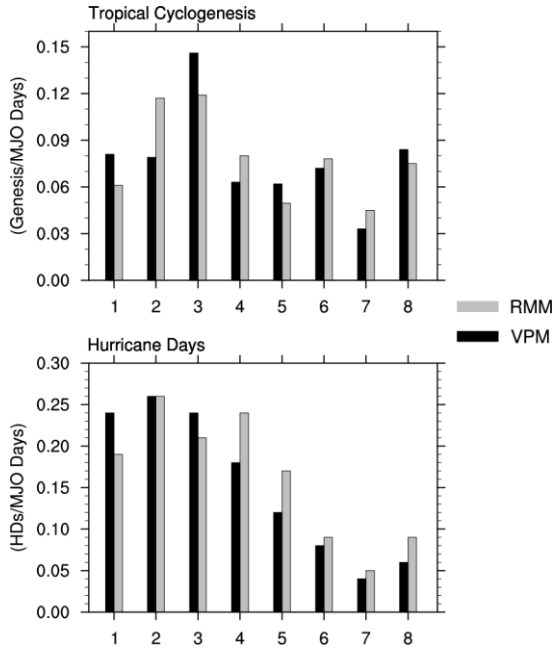

FIG. 4. (a) Normalized Atlantic genesis days and (b) normalized Atlantic HDs for each MJO phase for the VPM PCs (black) and the RMM PCs (grey) during the JJAS (1989-2009) season. Both (a) and (b) are normalized by the number of MJO days for each particular MJO Phase.

In Fig. 4a, the number of Atlantic tropical cyclogenesis events is divided by the number of MJO days for both sets of PCs. This normalization is necessary since the total number of MJO days is different for each phase and each index. Atlantic tropical cyclogenesis is observed to occur in all eight MJO phases for both sets of PCs. However, the most favorable phase for genesis is phase 3 for both the VPM and RMM PCs (14.6% and 11.9%, respectively, of the total number of events). The least favorable MJO phase for genesis is phase 7 for both the VPM and RMM PCs (3.3% and 4.5%, respectively, of the total number of events). Using the VPM PCs, tropical cyclogenesis is about four times more likely during phase 3 than during phase 7. Using the RMM PCs, tropical cyclogenesis is less than three times as likely to develop during MJO phase 3 with respect to MJO phase 7. Hence, the VPM index appears to detect a slightly stronger modulation of Atlantic tropical cyclogenesis than does the RMM index.

The MJO modulates Atlantic tropical cyclones because it impacts the large-scale environment over the tropical Atlantic. Therefore, we assume that the MJO might also affect the intensity of mature tropical cyclones there. In order to investigate whether Atlantic hurricane activity varies coherently with the VPM PCs, hurricane days (HDs) are binned for each MJO phase using the same MJO amplitude threshold as before (Fig. 4b). One HD is defined as a date when one or more tropical cyclones were active over the Atlantic and were associated with an intensity of greater than or equal to the Saffir and Simpson Scale Category 1 Hurricane (64 kt maximum sustained winds). Figure 9b shows the distribution of Atlantic hurricane days divided by the number of MJO days for each MJO phase for both of the VPM and RMM indices. The result shows that Atlantic hurricanes vary coherently with the MJO regardless of the MJO index that is used. Atlantic HDs are most favorable during phase 2 for both the VPM PCs and RMM PCs (26%). For the VPM PCs, there is a general reduction of normalized HDs after phase 2, with the minimum of HDs in phase 7 (4%). For the RMM PCs, the modulation is more noisy, with a second peak of occurring during phase 4 (24%).

Like the VPM PCs, a minimum of normalized HDs occur during phase 7 (5%) using the RMM PCs, but the overall modulation is not quite as strong. Hence, the VPM indices also show an enhanced capability to detect the modulation of HDs compared to the original RMM indices.

4. Conclusions

There is proven utility in having an index of the MJO that depicts its magnitude and location and that can be applied equally well in real-time, to historical records and to forecasts and hindcasts. The RMM index is such an index. However, some limitations to the RMM index exist, as noted in the introduction.

In particular, its use of OLR, a relatively noisy field with variability mostly limited to the Eastern Hemisphere, is one drawback that has been discussed in this paper. To this end, we have explored the potential benefits of a modified index of the MJO that uses VP200 rather than OLR to describe the convective/divergent component of the MJO but is otherwise similar.

The use of VP200 instead of OLR appears to better discriminate to the MJO signal during boreal summer and may potentially capture precursors of the MJO before a strong local signal in convection is evident. The inverse Laplacian used to calculate VP200 acts a smoother, which makes VP200 more sensitive to global-scale variations of convection/divergence rather than being concentrated on the Indo–Pacific warm pool like OLR. However, this increased sensitivity to convection in the Western Hemisphere comes at the expense of sensitivity in the Eastern Hemisphere, as well as during the boreal winter.

Although we have emphasized a possible benefit of modifying one component of the MJO index, this sort of MJO index, where by EOFs are calculated of equatorially averaged fields, is by no means the only approach worth pursuing. In fact, a general conclusion of this study is that there are alternative MJO indices that will have different sensitivities to the features of the MJO. These different indices may be more suitable for specific applications than is the RMM. To this end, we encourage and recommend exploration of alternative indices in order to promote a better understanding of the MJO and its global impacts.